Electrochimica Acta 215 (2016) 313–325

Contents lists available at ScienceDirect

Electrochimica Acta

journal homepage: www.elsevier.com/locate/electacta

Thermal and Chemical Stability of *n*-Hexadecanethiol Monolayers on Au(111) in O_2 Environments

Fernando P. Cometto[a,*], Gustavo Ruano[b,c,1], Federico A. Soria[d], C. Andrea Calderón[a,2], Patricia A. Paredes-Olivera[d], Guillermo Zampieri[b,c], E. Martín Patrito[a,*]

[a] Departamento de Fisicoquímica, Instituto de Investigaciones en Fisicoquímica de Córdoba (INFIQC), Facultad de Ciencias Químicas, Universidad Nacional de Córdoba, Córdoba, Argentina
[b] Centro Atómico Bariloche, Comisión Nacional de Energía Atómica, Bariloche, Argentina
[c] Instituto Balseiro, Universidad Nacional de Cuyo, Bariloche, Argentina
[d] Departamento de Matemática y Física, Instituto de Investigaciones en Fisicoquímica de Córdoba (INFIQC), Facultad de Ciencias Químicas, Universidad Nacional de Córdoba, Córdoba, Argentina

ARTICLE INFO

Article history:
Received 23 June 2016
Received in revised form 15 August 2016
Accepted 24 August 2016
Available online 26 August 2016

Keywords:
Alkanethiols
Self-assembly
Au
Stability
DFT
Molecular dynamics

ABSTRACT

Understanding the mechanisms of degradation of self-assembled monolayers (SAM) is required for their use in molecular devices and in general in long term applications. In this context, we investigated the thermal and chemical stability of *n*-hexadecanethiolate (C16T) monolayers on Au(111) exposed to O_2. The degradation of the monolayers was followed by electrochemical (EC) techniques, surface enhancement Raman spectroscopy (SERS) and high resolution photoemission spectra (HR-XPS). The C16T monolayers were heated both under N_2 and O_2 flux up to 480 K for different times. The degradation of the SAM in the presence of O_2 is characterized by the appearance of oxidized sulfur species and sulfur atoms on the surface. The formation time in the dipping solution also affects the thermal stability of the monolayer. Molecular dynamics (MD) simulations and density functional theory (DFT) calculations were performed to elucidate the possible degradation mechanisms. MD shows that O_2 molecules easily penetrate the monolayer reaching the Au surface. The DFT calculations identified two oxidation mechanisms which involve the S atom and the alpha carbon of the alkylthiolate. Both mechanisms are very exothermic. The oxidation of the sulfur atom produces a sulfinate which does not alter the monolayer structure. On the contrary, the oxidation of the alpha carbon induces the breakage of the S—C bond, the adsorption of atomic S and the desorption of the alkyl chain as an aldehyde.

1. Introduction

The stability of self-assembled monolayers is a challenging issue for applications where long-term use or high temperatures are required [1]. The understanding of the mechanisms of SAM degradation provides valuable information for the development of two-dimensional devices such as the lab-on-a-chip or 3D nano materials such as monolayer-protected nanoparticles. The interest of using SAMs as platforms for biological studies has motivated several studies related to the oxidation of the sulfur headgroup [2–4]. The gold–thiolate bond degrades when exposed to air [1,4–7]. The presence of oxidized sulfur was confirmed in several studies which found sulfinates and sulfonates for alkanethiols on the gold surface [8,9] as well as on gold nanoparticles [10]. Several reports have concluded that the oxidation of alkanethiols occurs extremely rapidly through ozone exposure [5,11–13].

The thermal stability of SAMs has been mainly investigated under vacuum conditions using thermal desorption spectroscopy (TPD). The nature of the organic chain [14,15], the preparation method [16] and the substrate morphology [17] influence the thermal stability. Densely packed short chain alkanethiols dimerize and desorb as disulfides with increasing temperature [17]. The breakage of the S—C bond occurs at high temperatures [18,19].

* Corresponding authors.
E-mail addresses: fcometto@fcq.unc.edu.ar (F.P. Cometto), martin@fcq.unc.edu.ar (E. M. Patrito).
[1] Present address: Instituto de Física del Litoral (IFIS), Santa Fe, Argentina.
[2] Present address: Instituto de Investigaciones Fisicoquímicas Teóricas y Aplicadas (INIFTA), La Plata, Argentina.

http://dx.doi.org/10.1016/j.electacta.2016.08.119
0013-4686/

A difficult task in thermal studies of SAMs is to quantify the amount of sulfur atoms and alkanethiols left on the surface. The sulfur in thiolate molecules is detected in TPD by the appearance of the masses corresponding to the molecular thiol or thiolate ions at around 450 K [17]. However, when the molecules decompose during a TDS experiment, one important issue is to distinguish between the cracking of the molecules in the quadrupole mass spectrometer upon ionization and the decomposition of the molecules on the surface. The appearance of sulfur atoms on the surface, originating from the breakage of the S—C bond of the alkanethiol, is evidenced indirectly by the desorption of H_2S molecules at high temperatures (around 650 K) [15]. The hydrogen atoms of H_2S originate from the partial dehydrogenation of the alkyl chains at high temperatures. Electrochemistry provides a valuable tool to quantify the sulfur content of the surface from reductive desorption current peaks of sulfur and alkanethiolate species as we have shown in previous works [20,21].

In the present work we investigate the thermal and chemical stability of C16T monolayers on Au(111) exposed to different doses of O_2 in order to elucidate the mechanisms of oxidation. We considered heating under a flux of N_2 and O_2 as well as under a low pressure of O_2. The monolayers were prepared by the dipping method and we show that the dipping time in the presence of O_2 has a profound effect on the monolayer thermal stability. EC techniques, SERS and HR-XPS are used to identify and quantify the surface products after the thermal treatment. The decomposition of the monolayer is characterized by the appearance of oxidized sulfur species as well as atomic sulfur on the surface. Molecular dynamics simulations are performed to investigate the diffusion of O_2 within the monolayer whereas DFT calculations are used to calculate the energetics of the initial stages of oxidation of the alkanethiol.

2. Experimental

2.1. Gold substrates

We used three types of Au substrates. For all the electrochemical measurements we used a crystal, 4 mm in diameter, oriented better than 1 degree towards the (111)-face and polished down to 0.03 μm (MaTeck, Jülich, Germany). Before the assembly process, the crystal was annealed in a hydrogen flame for two minutes, cooled under constant N_2 flux, and put in contact with water after one minute. For the XPS measurements we used Au films evaporated on borosilicate glass (250 nm thick, Arrandee). Before the assembly process the Au films were immersed in a hot piranha solution (H_2SO_4:H_2O_2, 70:30) during 30 seconds and then copiously washed with Milli-Q water. Finally, they were annealed in a butane flame for two minutes and then cooled down to room temperature under constant N_2 flux. For SERS measurements we used films with roughened surfaces prepared by applying a voltage step of 2.4 V during 10 min in 0.5 M H_2SO_4 solution and then, a linear potential sweep at 0.02 Vs^{-1} from 2.4 to −0.6 V [22,23].

2.2. Preparation of SAMs

N-hexadecanethiol was purchased from Sigma-Aldrich. Pure ethanol (Baker) was used as solvent. Chemicals were used as received without further purification. The samples were immersed in 1.0 mM deoxygenated solutions at room temperature by different periods of time. After the monolayers were formed the substrates were rinsed copiously with ethanol and Milli-Q water and blown dry with N_2.

2.3. Thermal treatment

After the SAMs formation, substrates were heated during 30 minutes (or different heating times at 458 K) at a fixed temperature in the range from 298 to 573 K (±5 K) under different conditions: a) N_2 atmosphere (where the partial pressure of O_2 is less than 4×10^{-2} mbar), b) in a low pressure chamber (with a partial pressure of O_2 less than 1×10^{-2} mbar), c) or in a O_2-saturated atmosphere. After thermal treatment the samples were quickly transferred (under N_2-rich atmosphere) to the electrochemical cell or to the vacuum chamber (for XPS measurements). Thermal treatments were always performed for freshly prepared monolayers after immersion times of 15 minutes or longer. Irrespective of immersion times, we obtained reductive desorption charges in the narrow range of 75–80 $\mu C/cm^2$ at room temperature. The smooth plots showing the variation of different monolayer properties with temperature indicate that the preparation procedure was very reproducible.

2.4. Cyclic voltamperometry and impedance spectroscopy

Cyclic Voltammograms (CV) and electrochemical impedance spectroscopy measurements were performed with a Solartron 1260 electrochemical interface and a three electrode cell with separate compartments for reference (Ag/AgCl (NaCl 3 M)) and a counter electrode (Pt wire). The 0.1 M KOH electrolyte was thoroughly deoxygenated by bubbling with N_2 prior to each experiment. Measurements were made at a sweep rate of 50 mV/s. Electrochemical Impedance spectra were recorded in the frequency range 1 Hz–10 kHz using a peak to peak signal amplitude of 0.01 V. Electrochemical measurements were performed at room temperature.

2.5. Photoelectron spectroscopy

The photoemission experiments were carried out at the D08A-SGM beamline of the Brazilian Synchrotron Light Laboratory (Campinas, Brazil). The pressure in the analyzer chamber was in the low 10^{-9} Torr range. Electron energy spectra were collected with a 150 mm hemispherical analyzer with its axis placed at 90 degrees from the light beam and in the plane of the light polarization. The samples were mounted with the surface normal lying in the plane of the photon beam and electron emission directions, and at 45 degrees from each direction.

The sample cleanliness was checked with survey spectra acquired with $h\nu = 600$ eV; only the characteristic peaks of Au, S and C were observed. Detailed S2p core-level spectra were measured at a photon energy of 300 eV. Before and after each spectrum we measured Au4f core-level spectra for count normalization and to calibrate the binding energies (BE) against that of the $Au4f_{7/2}$ core level at 84.0 eV. The S2p spectra were fitted with a linear background and three elemental components, each made of a pair of Voigt functions separated by 1.18 eV and fixed intensity ratio 2:1. The intensities, positions and Gaussian widths of the components were varied during the fittings; the Lorentzian width was kept fixed at 0.15 eV.

2.6. Surface-enhanced Raman spectroscopy

SERS experiments were performed with a Horiba LabRAM HR. The objective for laser illumination and signal collection was of a long working distance objective (8 mm) with a numerical aperture of 0.7 and a magnification of 100. The excitation line was from a 632.8 nm He-Ne laser, the power of the laser on the sample was about 5 mW.

3. Computational methods

3.1. Density Functional Theory calculations

Periodic Density Functional Theory (DFT) calculations were performed with the PBE functional [24] and ultrasoft pseudopotentials [25] using the Quantum Espresso code [26]. The one-electron wave functions were expanded in a plane wave basis set up to a kinetic energy cutoff of 30 Ry (180 Ry for the density). Brillouin zone integration was performed using a $(4 \times 4 \times 1)$ Monkorst-Pack mesh [27]. The periodic supercell approach was employed to describe a $2\sqrt{3} \times 3$ unit cell of the Au(111) surface containing the adsorbate molecules. The surface was modelled using a slab with four gold layers. We used an optimized lattice constant $a_0 = 4.1768$ Å for gold. The positions of all the adsorbate atoms as well as those of three two topmost Au layers were fully optimized up to a RMS force of 0.01 eV/Å. A vacuum thickness of 10 Å was introduced between the slabs. Due to the large alkyl chain of C16T, the DFT modelling was performed using hexanethiol. Four hexanethiolates were packed in the $2\sqrt{3} \times 3$ unit cell corresponding to a surface coverage of 0.33. The Climbing Image Nudged Elastic Band (CI-NEB) method was used to calculate energy profiles along reaction paths [28].

3.2. Reactive molecular dynamics calculations

The calculations were performed with the LAMMPS code [29] using the ReaxFF force field developed by van Duin, Goddard and co-workers [30,31]. This reactive force field provides an accurate description of bond breaking and bond formation during the MD simulations by employing a bond order/bond energy relationship. The force field employed (code name Au/C/S/O/H) was developed in previous works to describe the interaction between alkanethiols and the gold surface [32] combined with the parametrization for the interaction of O_2 with alkanes and the gold surface [33,34].

The Au(111) surface was represented by a slab with 4 layers containing 48 Au atoms in each layer. The cell was packed with 16 C16T species yielding a surface coverage of 0.33. The xyz cell dimensions were 20.0 Å × 17.3 Å × 10.0 Å. O_2 molecules were added in the free space between the thiolated Au slabs to investigate the O_2 diffusion within the monolayer. The slabs were thermalized in the canonical (NVT) ensemble at 300 K (Berendsen thermostat) for 1 ps using a time step of 0.1 fs with a temperature damping constant of 100 fs. Then the MD simulations were performed during 300 ps at 300 and 500 K.

4. Results

4.1. Characterization of C16T SAMs after thermal treatment

Fig. 1a shows the CV profiles recorded after a heating time of 30 minutes at different temperatures under N_2 flux. A freshly prepared monolayer was used at each temperature. Fig. S1 contains the CV profiles obtained after heating the monolayers at the highest temperatures. The reductive desorption (RD) current peak of the sample maintained at room temperature (RT) is characterized by a broad peak whose components A and B have potentials at −1.15 and −1.19 V, respectively (if the CV scan is performed at 10 mV/s, both components clearly resolve). When the potential scan is reverted, two well-defined readsorption peaks, A′ (−0.88 V) and B′ (−0.94 V) are observed. This voltammetric profile at room temperature is similar to that reported by Zhong et al. [35]. The RD profiles are almost unaltered up to 373 K. When the annealing temperature increases from 403 K to 423 K, the RD current peak decreases; indicating a decrease in the C16T coverage which is also detected in the oxidative readsorption peaks A′ and B′. In addition, the appearance of a new peak (C) at −0.94 V is observed at 423 K.

A peak at around −0.9 V has been observed for different SAMs [20,36,37] and has been attributed to the reductive desorption of

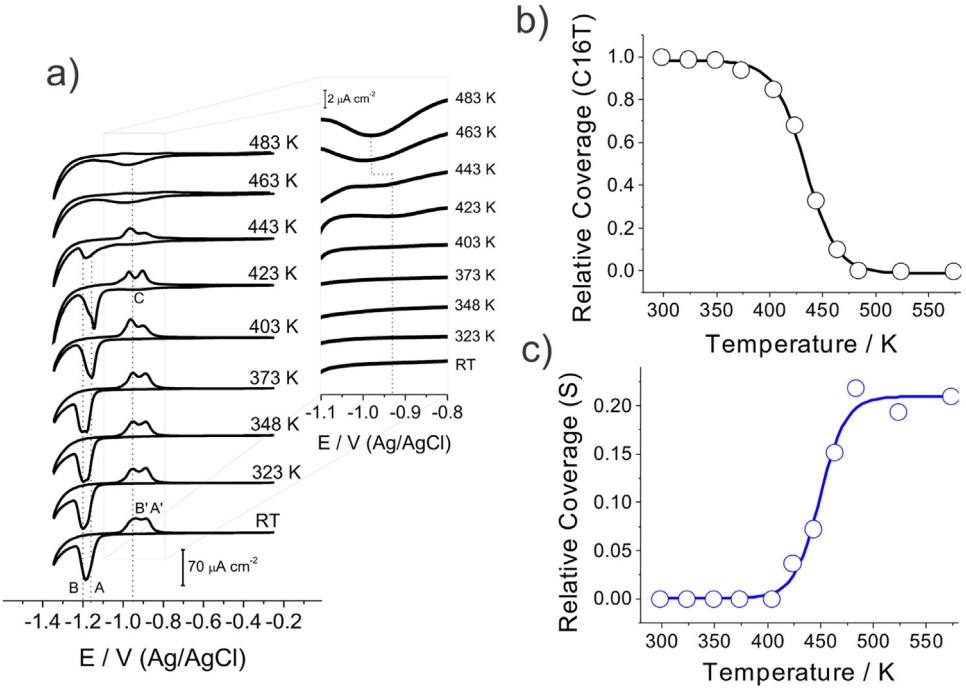

Fig. 1. a) Cyclic Voltammograms showing the reductive desorption of the adsorbed species remaining after thermal treatment (30 minutes under N_2 (4.8N) flux). Scan rate: 50 mV/s. Electrolyte: KOH 0.1 M. Reference electrode: Ag/AgCl (NaCl 3 M). Monolayers prepared after an immersion of 15 min in the forming solution. Surface coverage of adsorbed b) C16T and c) S species after heating. The thermal treatment always performed for a freshly prepared monoayer (15 min. immersion time).

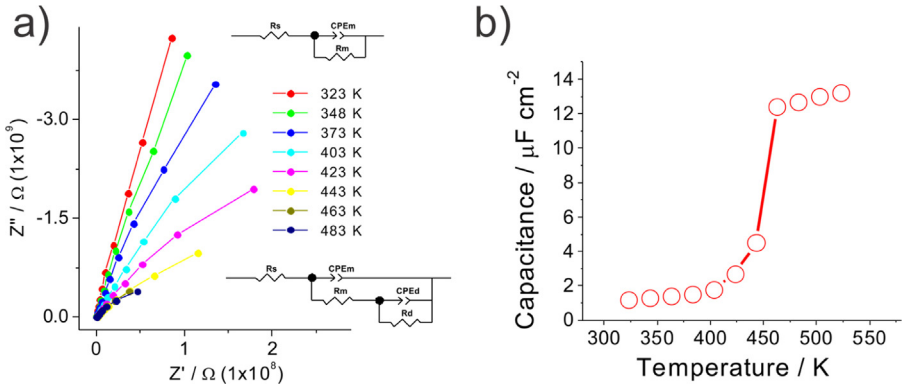

Fig. 2. a) Nyquist plots measured after heating freshly prepared monolayers (15 min. immersion time) during 30 minutes under N_2 (4.8N) flux b) Monolayer capacitance as a function of heating temperature. AC impedance measurements performed in KOH 0.1 M.

small amounts of atomic S. Peak C is not observed in freshly prepared C16T monolayers at RT indicating the absence of adsorbed S atoms on the surface as it is confirmed in the HR-XPS spectra. After heating at 443 K, a remarkable diminution of the RD peaks is observed together with an important increase of peak C (inset in Fig. 1a).

Fig. 1b and c shows the variation of surface coverage of alkanethiolate and sulphur species as a function of temperature. The reduction of alkanethiolates is a one-electron process [35] whereas two electrons are involved in the reduction of adsorbed sulphur atoms. A coverage of 1.0 corresponds to the reductive desorption charge of the freshly prepared monolayer (around 80 μC cm^{-2}) [38]. Fig. 1c shows that the appearance of sulphur on the surface coincides with the partial desorption of the monolayer (Fig. 1b). The amount of atomic sulphur at high temperatures was ~20% of the molecules in the freshly prepared monolayer. This indicates that upon a heating time of 30 minutes, ~80% of the C16T monolayer desorbed and the remaining ~20% decomposed via cleavage of the S—C bond.

Fig. 2a shows Nyquist plots of thermally treated C16T monolayers. At the lowest temperatures, the spectra were fitted with a circuit having a constant phase element (CPE) in parallel with the monolayer resistance R_m and with the solution resistance R_s in series. At the highest temperature we used a circuit which is usually employed for defective monolayers [20]. The general trend shown in Fig. 2b indicates an increase of the monolayer capacitance with the increase in the temperature. At 323, 348 and 373 K, the CV profiles in Fig. 1a show no major changes, indicating that the monolayer integrity is preserved. However, at these temperatures the monolayer capacitance steadily increases. The increase in capacitance in this temperature range is interpreted as decrease in the monolayer thickness according to the parallel plate capacitor formula. The decrease in thickness has been reported for alkyl monolayers on different substrates as a consequence of the disordering of the monolayer by an increased formation of gauche defects at high temperatures [39,40]. From 403 K, the monolayer decomposition is evident in the CV profiles and the increase in capacitance is more pronounced as shown in Fig. 2b. At these temperatures the changes in capacitance are attributed to the partial desorption/decomposition of C16T molecules with the remaining molecules probably in a lying-down configuration [41] as a consequence of the decrease in surface coverage.

Surface enhanced Raman scattering (SERS) has been extensively utilized as a major tool for unveiling the vibrational characteristics of adsorbents on noble metal surfaces owing to its enormous signal enhancement effect, even at very low concentration of species. Fig. 3a shows the SERS spectra in the 125 to 300 cm^{-1} and 2750 to 3000 cm^{-1} regions for C16T adsorbed onto black gold surfaces after 30 min of annealing at different temperatures under

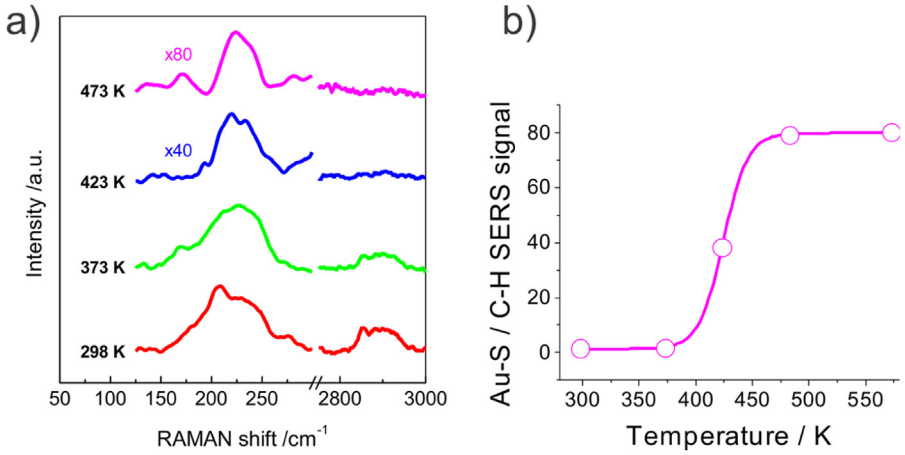

Fig. 3. a) SERS spectra for C16T adsorbed onto black gold surfaces after thermal treatment (30 minutes under N_2 (4.8N) flux). Only Au—S stretching (around 220 cm^{-1}) and C—H stretching (centred at 2900 cm^{-1}) regions are shown. For convenience, the intensities were normalized to the area of the Au—S signal obtained at 298 K. b) Au—S/C—H ratio of SERS signals as a function of temperature. The thermal treatment always performed for freshly prepared monoayers (15 min. immersion time).

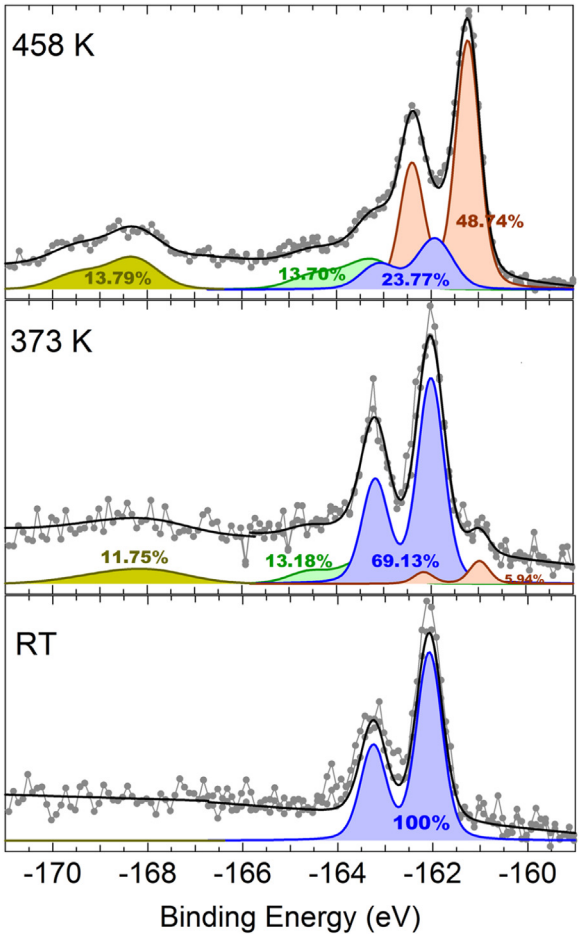

Fig. 4. HR-XPS spectra showing the S2p region at RT and after thermal treatment (30 min. heating under an O_2 partial pressure less than 1×10^{-2} mbar). The thermal treatment always performed for a freshly prepared monoayer (15 min. immersion time).

N_2 flux. The signal at around 220 cm^{-1} corresponds to the Au—S stretching meanwhile the other ones are associated to C—H stretching of the $—CH_2$ and $—CH_3$ groups presents in the alkanethiol chains [42–44]. For convenience, the intensities were normalized to the Au-S signal area obtained at 298 K. The occurrence of the signals around 220 cm^{-1} indicates that the thiolate bond may be tilted to the gold surface. At room temperature, both signals are present and decrease as the temperature increases. At 423 K both signals decrease abruptly and the signal corresponding to C—H almost disappears. Fig. 3b shows the Au—S/C—H area ratio vs annealing temperature. At room temperature the Au—S/C—H area ratio is 1.6, which remains almost constant even when the sample is annealed at 373 K. At higher temperatures, the C—H signals decrease significantly and consequently the area ratio (accounting for the occurrence of S and C atoms) increases to 40 and 80 at 423 K and 473 K, respectively (Fig. 3b). This result shows strong evidence that a fraction of molecules decompose at high temperatures leaving S atoms on the surface.

HR-XPS was used to characterize the nature of adsorbed species after the thermal treatment of freshly prepared monolayers. Fig. 4 shows the S2p spectra at RT, 373 and 458 K and Table 1a contains the fitted parameters of the corresponding peaks (binding energy, peak width and percentage of each component). The S2p spectrum of the pristine SAM at RT is mainly composed of a single narrow doublet (*fwhm* = 0.5 eV) with the $2p_{3/2}$ peak at 162.1 eV, which corresponds to adsorbed thiolates [45,46]. The S2p spectrum of the sample annealed at 373 K is similar to that measured at RT; the main change is an overall decrease of the intensities reflecting a partial desorption of the SAM, in good correspondence with the result of the CV experiment. The small component (13.2%) at around 163.5 eV is attributed to physisorbed species. However, there are two minor changes that deserve special attention: one is the growth of spectral intensity in the region around 168 eV where the emission from oxidized S species is expected [47]; the other is the appearance of a new feature, barely visible in this spectrum, at around 161 eV, which is attributed to S atoms chemisorbed at the hollow sites of the Au(111) surface [48] (see Table 1a).

The S2p spectrum of the sample annealed at the highest temperature (458 K) exhibits one important change: the dominant component is now the one at 161 eV (Table 1a). This change indicates clearly that annealing at 458 K produced sulfur atoms and an almost complete disappearance of the thiol layer, in full agreement with the electrochemical (Fig. 1a) and SERS (Fig. 3a) results. The component at around162 eV, previously assigned to the chemisorbed thiolates must be reassigned. We ascribe it to S atoms chemisorbed in other adsorption sites, following the assignment of Rodríguez et al. [48] who found the feature at 162 eV even at low S coverages on Au(111). Another change to be noted is the increase of the intensity in the region around 168 eV, denoting a further increase of oxidized S species on the surface [47].

In conclusion, the changes exhibited by the S2p spectra confirm the picture that the annealing under low partial pressure of O_2 (less than 1×10^{-2} mbar) causes a) the desorption of thiolates, b) the

Table 1
Peak deconvolution of S2p spectra measured after heating monolayers prepared by the immersion method during a) 15 minutes and b) 24 h in a 1 mM solution of C16T. The fitting parameters are the peak binding energy (BE), Gaussian width (G. width) and the percentage of each component. Four elemental components were considered. Each component contains a pair of Voigt functions separated by 1.18 eV and fixed intensity ratio 2:1. The intensities, energies and Gaussian widths of the components were varied during the fittings; the Lorentzian width was kept fixed at 0.15 eV.

a) 15 minutes

	RT	373 K				458 K			
BE (eV)	−162.1	−161.0	−162.0	−163.4	−167.9	−161.2	−161.9	−163.3	−168.3
G. width (eV)	0.56	0.41	0.58	1.00	1.86	0.52	0.81	1.14	1.16
%	100.0	5.9	69.1	13.2	11.8	48.7	23.8	13.7	13.8

b) 24 hours

	RT			458 K			
BE (eV)	−162.1	−163.4	−167.9	−161.2	−161.9	−163.4	−168.2
G. width (eV)	0.58	0.63	0.84	0.52	0.84	1.16	1.05
%	82.9	5.8	11.3	51.5	19.1	14.7	14.7

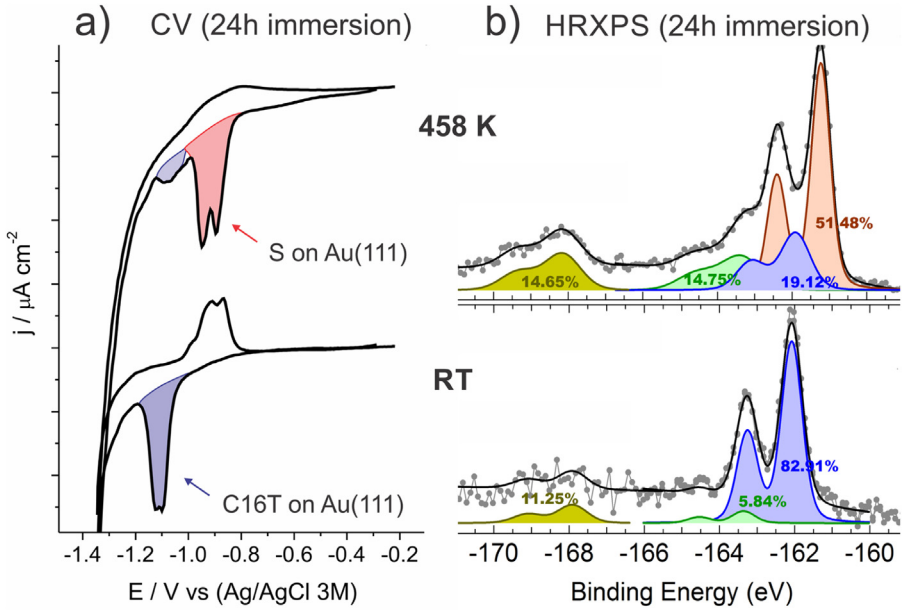

Fig. 5. a) Cyclic Voltammograms and b) photoemission spectra showing S2p region of a pristine C16T monolayer prepared during 24 h immersion. The subsequent thermal treatment was performed under N_2 (4.8N) flux during 30 minutes. CV profiles performed at 50 mV/s. Electrolyte: KOH 0.1 M. Reference electrode: Ag/AgCl (NaCl 3 M).

cleavage of S—C bonds leaving atomic S on the surface and c) the appearance of oxidized S species.

4.2. Influence of formation time on the stability of SAMs

The influence of the dipping time and the type of solvent of the forming solution on the structure of SAMs has been investigated by electrochemistry, STM, and XPS to determine the influence of these parameters on the SAM structure [49,50]. However, the influence of these parameters on the thermal stability of SAMs has been less investigated. The influence of the ambient exposure on the thermal stability of a mercaptoundecanoic acid SAM has been investigated by TPD. For this aged SAM, only a small fraction of the molecules desorbed intact, thus revealing important changes in the monolayer structure [15].

We found that the dipping time in non-deoxygenated forming solutions has a profound influence on the thermal stability of the C16T monolayer. Fig. 5 shows the CV profiles and XPS spectra of C16T prepared by immersing the gold substrate in ethanolic solution during 24 hours. Table 1b contains the corresponding peak deconvolution parameters. We compare the thermal response after keeping the sample during 30 minutes under N_2 flux at RT and 458 K.

The reductive desorption profile at room temperature (Fig. 5a) does not show any major differences with that of Fig. 1a corresponding to a dipping time of 15 min. The CV profile in Fig. 5a has a peak potential at -1.16 ± 0.03 V and a reductive desorption charge of $\sim 80\ \mu C/cm^2$ (blue area). However, remarkable differences are observed in the CV profile after heating at 458 K: the amount of S atoms increases up to 60-70% of the total coverage (red area) and only a small amount of C16T species remain on the surface (blue area).

The S2p spectrum at RT (Fig. 5b) is dominated by the thiolate component at 162.1 eV (82.9%). Besides the broad component at around 163.4 eV due to physisorbed species (5.8%) we also observed a signal at a higher BE of 167.9 eV that denotes the presence of some oxidized S species even for this fresh sample. This was not observed with a dipping time of 15 min. (Fig. 4). After annealing at 458 K, the dominant feature is the component at 161.2 eV (51.5%) assigned to S atoms adsorbed on hollow sites. The component at high BE assigned to oxidized S species grows in intensity and shifts to larger BEs (Table 1b), indicating an increase of oxidation states at 458 K

Oxidative readsorption peaks are very helpful to discriminate whether a previous reductive desorption peak corresponds to sulfur or to alkanethiolates. When the reduction peak corresponds to long chain alkanethiolates, the corresponding oxidative readsorption peak is observed in the reverse scan due to the low diffusion coefficient of the alkanethiolates. On the contrary, when adsorbed sulphur is reductively desorbed, it rapidly diffuses into the electrolyte and virtually no readsorption peak is detected when the potential scan is reversed. This is observed in Fig. 5a where a clearly defined double peak is observed during the oxidative readsorption at RT and only a small and diffuse peak is observed at 458 K. This confirms that the reductive desorption after heating at 458 K corresponds to S species on the surface. In conclusion, the thermal behavior of a C16T monolayer formed by longer dipping times is characterized by the appearance of adsorbed S atoms as well as minor amounts of oxidized sulfur species.

Monolayers prepared in a 1 mM C16T solution using immersion times of 15 minutes and 24 hours were subsequently heated at 458 K for different times under a N_2 flow. After the heating procedure CV profiles were obtained as shown in Fig. 6a and b. The relative surface coverage of sulfur and thiolate species was calculated by integrating the corresponding reductive desorption current peaks as shown in Fig. 6c. The decrease of the thiolate surface coverage is more pronounced for the longest immersion times. After a heating time of 60 minutes, virtually no thiolates are observed for the monolayers formed by 24 hours dipping, whereas for the monolayer formed by 15 min. dipping, the thiolate surface coverage is around 30%. The disappearance of thiolates correlates with the appearance of sulfur atoms. For monolayers formed by 24 hours of dipping, the sulfur surface coverage is 70% of the sulfur originally present as thiolate after a heating time of 60 minutes. This indicates that 70% of the thiolate molecules decomposed whereas the remaining 30% desorbed from the surface. The

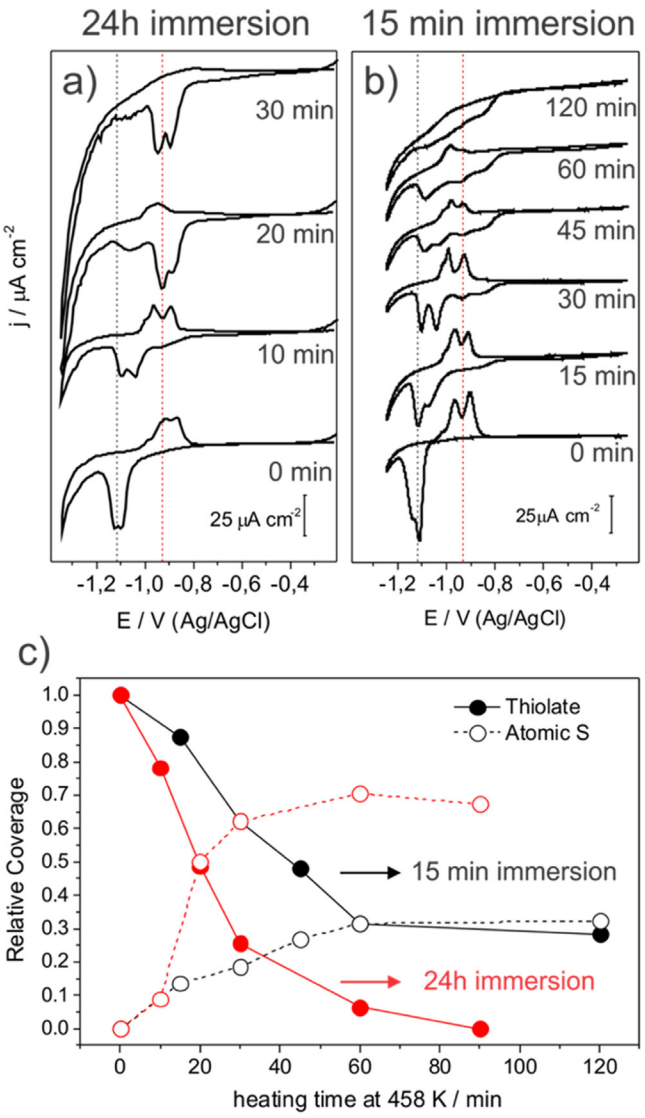

Fig. 6. Cyclic Voltammograms a-b) and relative surface coverage c) of thiolate and sulfur species as a function of heating time at 458 K for C16T monolayers prepared by dipping times of 15 min and 24 hours. Thermal treatment under N_2 (4.8N) flux. Solid lines for C16T and dashed lines for S atoms. Forming solutions were not deoxygenated. Scan rate: 50 mV/s. Electrolyte: KOH 0.1 M. Reference electrode: Ag/AgCl (NaCl 3 M).

reversed trend is observed at the shortest dipping time of 15 minutes where only 30% of the molecules decomposed.

4.3. Thermal stability in O_2-rich conditions

In the previous experiments, the thermal treatments were performed under the small amounts of O_2 in the N_2 flux. In this section, we investigate the thermal stability of samples prepared after 15 minutes immersion in C16T solutions and then heated under a flux of pure O_2. The freshly prepared monolayers were exposed to O2 at RT, 313 K and 373 K during 30 minutes and then the CV profiles were recorded. Fig. 7a shows that heating at 313 K during 30 minutes leads to the appearance of a well-defined peak at −0.91 V (indicating the presence of S atoms on the surface) and to a decrease of the characteristic reductive desorption peak of C16T. The relative area of the peaks after heating at 373 K indicate that S atoms cover almost the entire surface and that only a small amount of pristine C16T molecules remain on the surface. Fig. 7b shows the variation of the reductive desorption charge for thiolate and sulfur species as a function of temperature. Up to 373 K the decrease of the thiolate charge correlates with the increase in the reduction charge of atomic sulfur. Considering that the reductive desorption involves one electron per thiolate and two electrons per sulfur atom, we find that the total sulfur content of the surface (thiolates + sulfur) remains constant up to 373. At the highest temperature both C16T and S atoms desorb from the surface (Fig. 7b).

In summary, the thermal stability of the C16T monolayer greatly decreases in the presence of O_2 which induces the formation of sulfur atoms and oxidized sulfur species on the surface. This implies that oxygen molecules may diffuse through the monolayer reaching the sulfur atoms of alkylthiolates at the Au/SAM interface. In order to gain a deeper insight into the processes that may contribute to the decomposition of the monolayer, we performed MD simulations to investigate the diffusion of O_2 and DFT calculations to characterize the energetics of the possible reactions leading to the formation of both S atoms and oxidized sulfur species on the surface.

4.4. Molecular dynamics simulations

Fig. 8 shows different snapshots illustrating the main features of the monolayer structure at 500 K. The top view in Fig. 8a shows that the position of the S atoms deviate from the average separation of 5 Å in the $(\sqrt{3} \times \sqrt{3})R30^\circ$ structure. The S atoms have an appreciable surface mobility and they may be observed on hollow, bridge and ontop surface sites. The red circle in Fig. 8a shows the formation of a disulfide bond between the S atoms of adjacent thiolates (with an interatomic separation of 2.15 Å) in agreement with the dialkyldisulfide desorption mechanism observed experimentally [17]. The large amount of gauche conformational disorder in the alkyl chains can be observed in the side views of Fig. 8b and c. Gauche defects are observed in all positions of the alkyl chain and produce a decrease in the thickness of the monolayer. This is consistent with the increase in the monolayer capacity observed experimentally before the desorption process begins as discussed above in relation to Fig. 2. Fig. 8b shows an example of an alkyl chain with the first C atoms in an all-trans configuration with gauche defects at the end of the molecule, whereas Fig. 8c shows a molecule with several gauche defects along the alkyl chain and having the terminal methyl group pointing towards the surface. At 300 K the amount of gauche defects is lower than at 500 K as it can be seen in Fig. S2.

We next introduced 5 oxygen molecules in the vacuum region above the SAM and as soon as they became in contact with the monolayer they penetrated and were never released during the simulation time as shown in Fig. 9. Oxygen molecules occupy the void volumes generated by the disorder of the alkyl chains (Fig. 9a). The diffusion of O_2 through the monolayer towards the gold surface takes over 110 ps of simulation time. Fig. 9b shows a snapshot in which one O_2 molecule has reached the gold surface.

These results show the ability of the monolayer to dissolve oxygen and are in agreement with MD simulations of O_2 within lipid bilayers which show a high solubility for oxygen (up to mM concentrations) dictated by the effect of hydrophobicity and accessible free volume [51,52]. Dissolved O_2 induces the formation of gauche defects in the alkyl chains. This is clearly observed when comparing the monolayer structure with and without O_2, as shown in Fig. S3 in the Supporting Information. In conclusion, oxygen molecules get trapped within the monolayer which increases the probability of further reactions at the Au/SAM interface

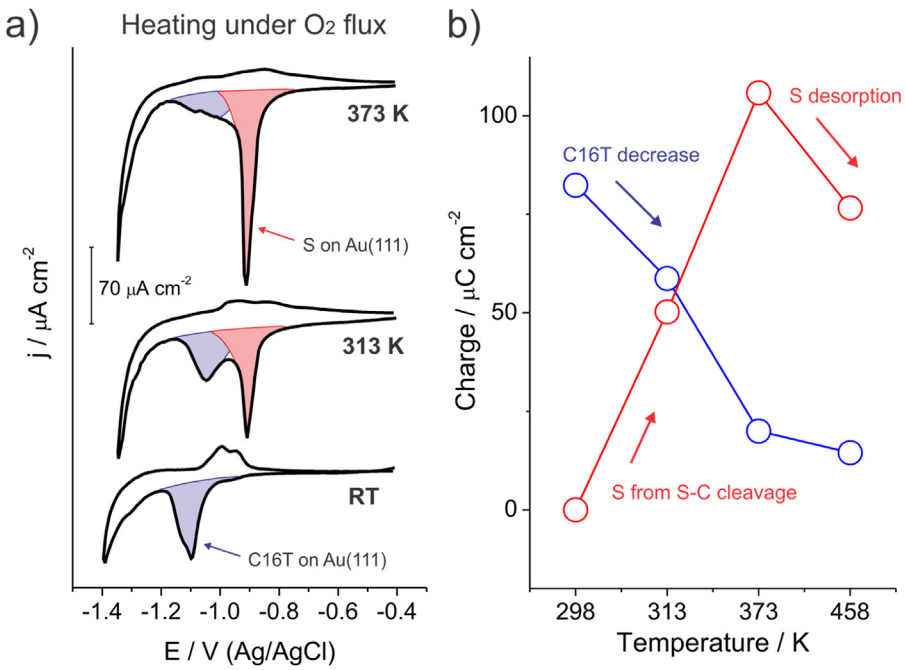

Fig. 7. a) Cyclic Voltammograms and b) reductive desorption charges measured after heating freshly prepared monolayers (15 min. immersion time) during 30 minutes under a flux of pure O_2 (4.8N). Scan rate: 50 mV/s. Electrolyte: KOH 0.1 M. Reference electrode: Ag/AgCl (NaCl 3 M).

4.5. DFT calculations

The energetics of the oxidation reactions at the SAM/Au interface were investigated by DFT starting with the equilibrium structure of an O_2 molecule within a C6T monolayer, as shown in Fig. 10a and b. The energy of this structure is taken as the reference. We next considered the initial stages of oxidation of the S and alpha C atoms of the hexanethiolate species within the monolayer using a $2\sqrt{3} \times 3$ unit cell with four molecules.

The first step in the oxidation of the S atom produces a RSOO species (Fig. 10c) in an endothermic reaction with $\Delta E = 6.6$ kcal/mol. This intermediate is bound to the surface by the S atom (S—Au bond distance of 2.51 Å) and the terminal O atom (O—Au bond distance of 2.29 Å), which lie approximately on top of gold atoms (Fig. 10c). In the next step the O atoms rearrange producing a sulfinate (Fig. 10d) which is bicoordinated to the surface via both O atoms (average O—Au bond distance of 2.41 Å). The formation of the sulfinate from the peroxo intermediate (Fig. 10c) is very exothermic with $\Delta E = -69.4$ kcal/mol, indicating that the former is a very stable species on the surface. The overall reaction, taking as a reference the O_2 molecule within the monolayer (Fig. 10a), has $\Delta E = -62.8$ kcal/mol.

Combustion reactions of alkanes are initiated with a hydrogen abstraction by O_2 generating an alkyl radical and the OOH species [53]. As the degrees of freedom are restrained within the SAM, the OOH radical may recombine with the radical left on the C atom to yield an intermediate with a peroxide group. In a previous work dealing with the mechanism of oxidation of alkanes grafted on Si (111) [54] we found that the first intermediate produced after the hydrogen abstraction reaction has the form —C—(OH)—O whereas the H atom originally bound to C is transferred to the approaching O atom of the O_2 molecule. From this intermediate two reaction paths may follow: the H atom can bind to the terminal O atom giving rise to a —C—O—OH species (this step has a low energy barrier of 6.3 kcal/mol on the Si surface [54]) as shown in Fig. 10e or the O—O bond may break giving rise to a —COH species and an O atom adsorbed on the Au(111) surface (Fig. 10f).

The equilibrium structure of the —COOH moiety shown in Fig. 10e has the OH group pointing towards the negatively charged S atom of the adjacent thiolate and the hydrogen bond has a length of 1.94 Å. The formation of the peroxo group is exothermic with $\Delta E = -30.0$ kcal/mol. The O-O bond in peroxides is a relatively weak bond and it may undergo cleavage to generate an alkoxy radical which decomposes to an aldehyde. We enlarged the O—O bond in the structure of Fig. 10e by 1.0 Å and then performed the geometry optimization. The system evolved to the equilibrium structure shown in Fig. 10g where significant atomic rearrangement has occurred: the breakage of the O—O bond led to the formation of an aldehyde group and the breakage of the S—C bond. The aldehyde molecule desorbs from the surface whereas the adsorbed products are the S atom and the hydroxyl radical, both located on hollow sites on the the Au(111) surface (Fig. 10g). The formation of the aldehyde from the peroxo intermediate is exothermic with $\Delta E = -31.3$ kcal/mol and the whole reaction has $\Delta E = -61.3$ kcal/mol, taking as a reference the O_2 molecule within the SAM (Fig. 10a).

The reaction leading to the formation of the alcohol group (Fig. 10f) is exothermic with $\Delta E = -45.2$ kcal/mol. Fig. 10f shows that there is a short hydrogen bond of 1.47 Å between the OH group and the adsorbed O atom (negatively charged). We enlarged this OH bond by 1.0 Å and then performed the geometry optimization. We obtained the same structure as in Fig. 10g where the formation of the aldehyde takes place together with the breakage of the S—C bond. This reaction has $\Delta E = -16.1$ kcal/mol and it is expected to have a low activation energy barrier. In a previous work [37] we obtained an energy barrier of 5.6 kcal/mol for the equivalent reaction $SCH_2OH + O \rightarrow SCH_2O + OH$ in a study of methanethiol decomposition.

In summary, the sulfur atom and the alpha carbon atom may be oxidized by O_2 in reactions that are very exothermic and have comparable ΔE values of −62.8 and −61.3 kcal/mol, respectively. The oxidation of the sulfur atom produces an alkanesulfinate species bicoordinated to the surface by both O atoms. As shown in Fig. 10d, the exchange of the sulfur head group by the sulfinate

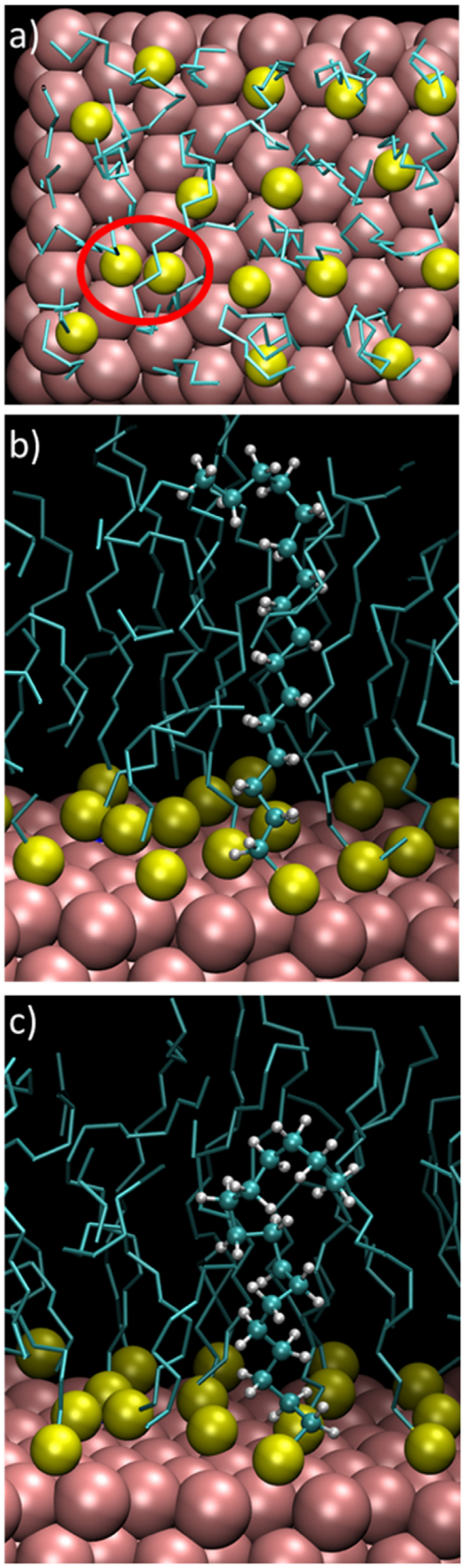

Fig. 8. Snapshots of MD simulations of a full coverage C16T monolayer at 500 K. a) Top view emphasizing the positions of S atoms. A disulfide species is enclosed in the red oval b) Side view showing the carbon chains in a wireframe representation for clarity, only one alkyl chain is shown explicitly. c) Side view showing explicitly an alkyl chain with an U-shaped conformation.

headgroup does not affect the integrity of the monolayer. However, the oxidation of the alpha carbon leads to desorption of the alkyl chain and leaves sulfur and OH species on the surface as a consequence of the breakage of the S—C bond.

5. Discussion

Under the conditions investigated in this work, the HR-XPS measurements showed that the formation of sulfur atoms prevailed over the oxidation of the thiolates to sulfinates, indicating that the oxidation of the alpha C atom of the alkyl chains is the most likely mechanism. For the oxidation reactions shown in Fig. 10 we did not compute the energy barriers of the different processes as it is very time consuming. However we can have an estimation from a previous work on the oxidation of carbon chains on Si(111), where we found energy barriers of around 40 kcal/mol for the formation of the —COOH moiety in a terminal methyl group [54] (the rate limiting step). The formation of the —COOH moiety in Fig. 10e may have a lower energy barrier as a consequence of the stabilization of the hydrogen abstraction reaction by the proximity of the metal surface and the hydrogen bonding with the S atom of neighboring thiolates. Therefore, the value of 40 kcal/mol can be taken as an upper limit.

In order to complete the picture of the energetics of the reactions that may take place at high temperatures we need to consider the direct desorption of alkanethiolates, the breakage of the S—C bond (in the absence of O_2) and the associative desorption of thiolates as disulfide molecules. The main contribution to the energy barrier for the direct desorption of an alkanethiolate radical originates from the breakage of the S—Au bond which has an energy of 44.3 kcal/mol in the case of a methanethiol monolayer [55]. The breakage of the S—C bond of a methanethiolate species within a full coverage monolayer has a barrier of 41.4 kcal/mol as can be seen in the energy profile as a function of the reaction path in Fig. S4 (we considered this short chain monolayer as the CI-NEB calculation is very time-consuming in the $2\sqrt{3} \times 3$ unit cell). For the desorption of a dimethyldisulfide molecule from a full coverage methanethiolate monolayer we obtained an energy barrier of 21.5 kcal/mol (Fig. S5). These values are to be compared with the barrier for the formation of the —COOH moiety, estimated to be lower than 40 kcal/mol.

This energetic picture implies that under moderate temperatures and high coverage conditions the disulfide formation mechanism, with a much lower energy barrier, will prevail over the direct desorption as it is observed experimentally [17]. For the other reactions, kinetic factors have to be considered to evaluate the reaction rate. The rate of direct desorption and the rate of S–C bond cleavage depend on the thiolate surface coverage whereas the rate of oxidation of the alpha carbon depends on the thiolate coverage as well as on the oxygen concentration. Therefore, high doses of O_2 may increase the rate of the latter reaction over the former reactions. This picture is consistent with our experimental observations. The fact that a large amount of atomic sulfur appears in the CV profiles recorded after heating the SAM under O_2 flux (Fig. 7) or after long immersion times (Fig. 6) implies that the decomposition of the monolayer occurs as a consequence of the oxidation of the alpha C atom (Fig. 10e).

It has been suggested in previous works that the metal substrate may play a role in the oxidation of the thiol molecules [1]. This becomes clear from Fig. 10. An important contribution to the high exothermicity of the oxidation reactions arises from the high affinities of the reaction products for the Au substrate: the S, OH and sulfinate species have high binding energies on the Au(111) surface.

The thermal stability of the C16T monolayer not only decreased upon exposure to O_2 but also when the dipping time in the forming

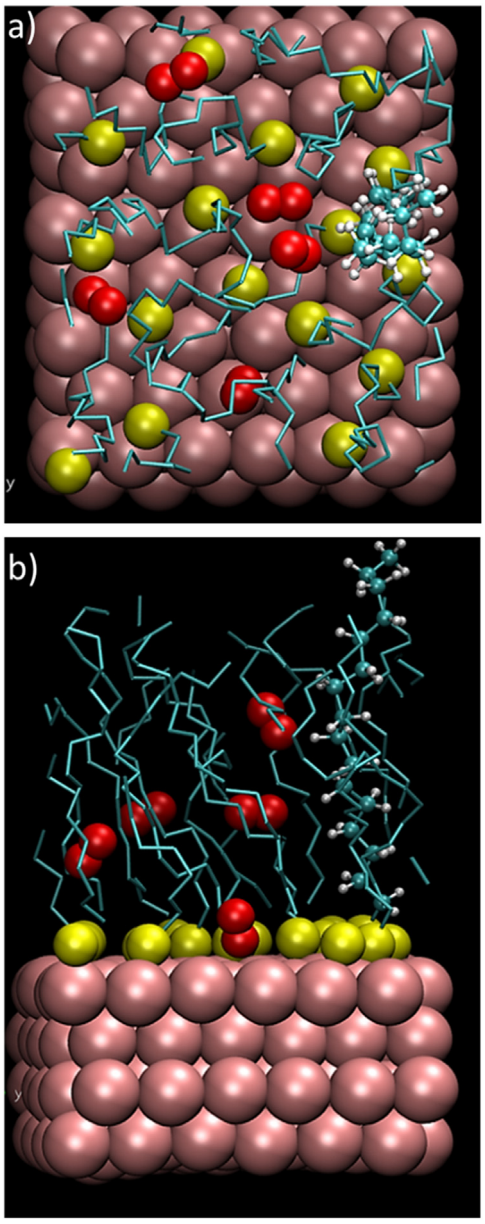

Fig. 9. Top a) and b) side views of snapshots of MD simulations of a full coverage C16T monolayer at 500 K containing 5 O_2 molecules. Carbon atoms of alkyl chains in wireframe representation except for one molecule which is shown explicitly.

solution was increased up to 24 hours. The molecular dynamics simulations provide some insights on this behavior. Fig. 9 shows that even at 500 K the O_2 molecules remain trapped within the monolayer as a consequence of hydrophobic interactions. Therefore, the longer the exposure of the monolayer to an environment containing O_2, the higher the amount of O_2 that may concentrate until saturation is reached. The oxygen-rich monolayer is expected to decompose according to the mechanisms shown in Fig. 10. This outlines the importance of keeping SAMs in inert atmospheres in applications which require a long term use. Another conclusion is that the amount of O_2 trapped within a monolayer is expected to be dependent on the nature of the carbon chain. Monolayers with long alkyl chains will have a high capacity to store O_2 molecules with the corresponding destabilizing effect. On the contrary, monolayer structures with a less dense molecular packing are expected to avoid the trapping of O_2. As an example of a molecular packing which prevents the penetration of O_2 we can mention the styrene-terminated Si(100)–2 × 1 surface: Si—CH_2—CH_2—phenyl. A molecular dynamics investigation showed that the phenyl ring rotates around the C—C bonds producing the repulsion of the impinging O_2 molecules [56].

6. Conclusion

The thermal and chemical stability of C16T monolayers on Au (111) were investigated under different preparation methods and thermal treatment conditions in the presence of O_2. The monolayers were heated under a low O_2 content in a N_2 flux as well as under an O_2 flux. The effect of the dipping time in the forming solution on the thermal stability was also investigated. The degradation of the monolayers was monitored using electrochemical, SERS and HR-XPS techniques. The photoelectron spectra revealed the presence of both sulfur atoms and oxidized sulfur species on the surface. The amount of electroactive sulfur and thiolate species was quantified from the charge of the corresponding reduction current peaks in the CV profiles performed after the heating procedure. Upon exposure to a flux of O_2, we observed a correlation between the disappearance of thiolates and the appearance of sulfur atoms on the surface up to a temperature of 373 K (Fig. 7).

The dipping time in non-deoxygenated solutions also had a profound effect on the thermal stability of monolayers heated during 30 min under a N_2 flux at 458 K. The electrochemical measurements revealed the disappearance of thiolates and the appearance of sulfur on the surface.

Molecular dynamics simulations were performed to investigate the structure of the monolayer at high temperatures and the interaction of O_2 with the alkyl chains. Oxygen molecules produce a disordering of the alky chains characterized by a large amount of gauche defects. Even at 500 K the O_2 molecules remain trapped within the SAM and can reach the gold surface. The destabilizing effect of long dipping times in the thermal stability of the C16T monolayer was attributed to a higher O_2 loading within the SAM. These results suggest that the nature of the carbon chain and consequently the type of packing of the molecules in the SAM are expected to influence the solubility of O_2 and therefore the chemical stability of the thiolates.

Density functional theory calculations were performed to unveil the possible mechanisms producing both sulfur atoms and oxidized sulfur species on the surface. The oxidation of the S atom of the thiolate produces a sulfinate in a very exothermic reaction with $\Delta E = -62.8$ kcal/mol (Fig. 10). The oxidation of the alpha carbon atom is responsible for the appearance of sulfur on the surface. It leads to the breakage of the S—C bond and desorption of the alkyl chain as an aldehyde. This reaction is also very exothermic with $\Delta E = -61.3$ kcal/mol. The high stability of the reaction products adsorbed on the Au surface is responsible for the exothermicity of these reactions showing that the substrate is effectively involved in the reactions leading to the degradation of the monolayer.

An energetic picture was presented including the energy barriers of the main reactions involved in the degradation of a monolayer: direct thiolate desorption, associative desorption as disulfides, S—C bond breakage and oxidation of alpha C atom. From purely energetic considerations, the most favored reaction is desorption as disulfides. However, in the presence of O_2 its concentration is a determinant factor in the rate of oxidation. The large amount of atomic sulfur observed after heating the SAM under O_2 flux or after long immersion times implies that the decomposition of the monolayer occurs predominantly via the oxidation of the alpha C atom.

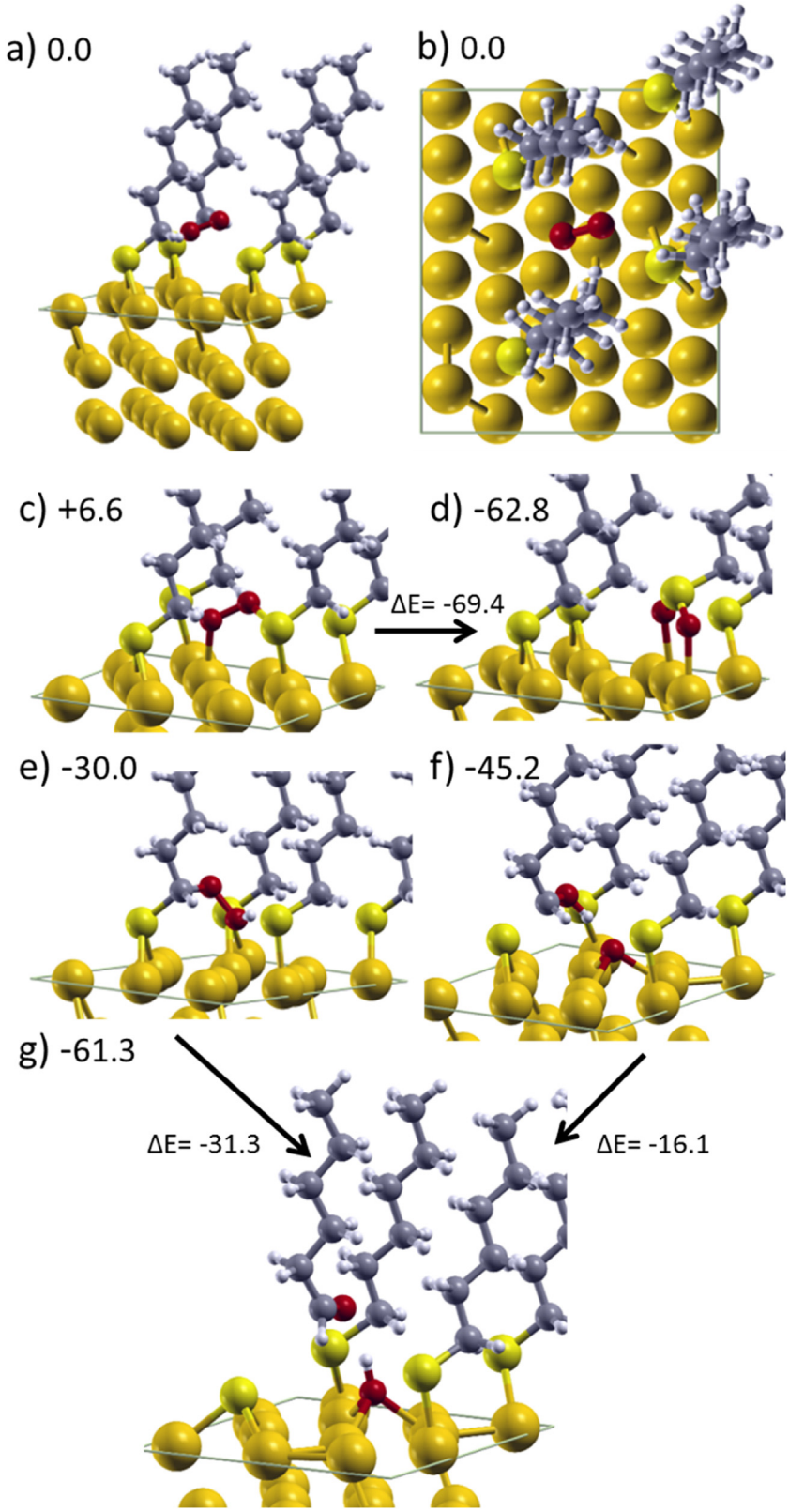

Fig. 10. Equilibrium structures of DFT calculations for a full coverage hexanethiolate monolayer in a $2\sqrt{3} \times 3$ unit cell. Side a) and top b) views of an O_2 molecule within the monolayer. The numbers indicate relative energies in kcal/mol taking this structure as the reference. c) —S—O—O— intermediate leading to the formation of d) sulfonite species. e) —C—O—OH intermediate, f) —C—OH + O_{ads} intermediate, g) desorbed aldehyde + O_{ads} + OH_{ads}.

Acknowledgments

Financial support from Conicet (PIP 5903), Secyt-UNC and Foncyt (PICT-2014-2199) is gratefully acknowledged. Raman facilities at "Laboratorio de Nanoscopía y Nanofotónica", INFIQC–CONICET/UNC, "Sistema Nacional de Microscopi'a", MINCyT, are gratefully acknowledged. This work used computational resources from CCAD – Universidad Nacional de Córdoba (http://ccad.unc.edu.ar/), which is part of SNCAD – MinCyT, República Argentina.

Appendix A. Supplementary data

Supplementary data associated with this article can be found, in the online version, at http://dx.doi.org/10.1016/j.electacta.2016.08.119.

References

[1] L. Srisombat, A.C. Jamison, T.R. Lee, Stability: A Key Issue for Self-Assembled Monolayers on Gold as Thin-Film Coatings and Nanoparticle Protectants, Colloids Surf. Physicochem. Eng. Aspects 390 (2011) 1–19.
[2] J.A. Jones, L.A. Qin, H. Meyerson, I.K. Kwon, T. Matsuda, J.M. Anderson, Instability of Self-Assembled Monolayers as a Model Material System for macrophage/FBGC Cellular Behavior, J. Biomed. Mater. Res. A 86A (2008) 261–268.
[3] G. Mani, D.M. Johnson, D. Marton, V.L. Dougherty, M.D. Feldman, D. Patel, A.A. Ayon, C.M. Agrawal, Stability of Self-Assembled Monolayers on Titanium and Gold, Langmuir 24 (2008) 6774–6784.
[4] T.M. Willey, A.L. Vance, T. van Buuren, C. Bostedt, L.J. Terminello, C.S. Fadley, Rapid Degradation of Alkanethiol-Based Self-Assembled Monolayers on Gold in Ambient Laboratory Conditions, Surf. Sci. 576 (2005) 188–196.
[5] M.H. Schoenfisch, J.E. Pemberton, Air Stability of Alkanethiol Self-Assembled Monolayers on Silver and Gold Surfaces, J. Am. Chem. Soc. 120 (1998) 4502–4513.
[6] A.B. Horn, D.A. Russell, L.J. Shorthouse, T.R.E. Simpson, Ageing of Alkanethiol Self-Assembled Monolayers, J. Chem. Soc. Faraday Trans. 92 (1996) 4759–4762.
[7] R.L. Garrell, J.E. Chadwick, D.L. Severance, N.A. McDonald, D.C. Myles, Adsorption of Sulfur Containing Molecules on Gold: The Effect of Oxidation on Monolayer Formation and Stability Characterized by Experiments and Theory, J. Am. Chem. Soc. 117 (1995) 11563–11571.
[8] J.R. Scott, L.S. Baker, W.R. Everett, C.L. Wilkins, I. Fritsch, Laser Desorption Fourier Transform Mass Spectrometry Exchange Studies of Air-Oxidized Alkanethiol Self-Assembled Monolayers on Gold, Anal. Chem. 69 (1997) 2636–2639.
[9] M.J. Tarlov, J.G. Newman, Static Secondary Ion Mass Spectrometry of Self-Assembled Alkanethiol Monolayers on Gold, Langmuir 8 (1992) 1398–1405.
[10] Y. Joseph, B. Guse, G. Nelles, Aging of 1,ω-Alkyldithiol Interlinked Au Nanoparticle Networks, Chem. Mater. 21 (2009) 1670–1676.
[11] K.L. Norrod, K.L. Rowlen, Ozone-Induced Oxidation of Self-Assembled Decanethiol: Contributing Mechanism for Photooxidation, J. Am. Chem. Soc. 120 (1998) 2656–2657.
[12] Y. Zhang, R.H. Terrill, T.A. Tanzer, P.W. Bohn, Ozonolysis Is the Primary Cause of UV Photooxidation of Alkanethiolate Monolayers at Low Irradiance, J. Am. Chem. Soc. 120 (1998) 2654–2655.
[13] Y. Zhang, R.H. Terrill, P.W. Bohn, Ultraviolet Photochemistry and Ex Situ Ozonolysis of Alkanethiol Self-Assembled Monolayers on Gold, Chem. Mater 11 (1999) 2191–2198.
[14] A. Turchanin, D. Käfer, M. El-Desawy, C. Wöll, G. Witte, A. Gölzhäuser, Molecular Mechanisms of Electron-Induced Cross-Linking in Aromatic SAMs, Langmuir 25 (2009) 7342–7352.
[15] J. Stettner, P. Frank, T. Griesser, G. Trimmel, R. Schennach, E. Gilli, A. Winkler, A Study on the Formation and Thermal Stability of 11-MUA SAMs on Au(111)/Mica and on Polycrystalline Gold Foils, Langmuir 25 (2009) 1427–1433.
[16] D. Käfer, G. Witte, P. Cyganik, A. Terfort, C. Wöll, A Comprehensive Study of Self-Assembled Monolayers of Anthracenethiol on Gold: Solvent Effects, Structure, and Stability, J. Am. Chem. Soc. 128 (2006) 1723–1732.
[17] T. Hayashi, K. Wakamatsu, E. Ito, M. Hara, Effect of Steric Hindrance on Desorption Processes of Alkanethiols on Au(111), J. Phys. Chem. C 113 (2009) 18795–18799.
[18] T. Ishida, N. Choi, W. Mizutani, H. Tokumoto, I. Kojima, H. Azehara, H. Hokari, U. Akiba, M. Fujihira, High-Resolution X-Ray Photoelectron Spectra of Organosulfur Monolayers on Au(111): S(2p) Spectral Dependence on Molecular Species, Langmuir 15 (1999) 6799–6806.
[19] T. Ishida, M. Hara, I. Kojima, S. Tsuneda, N. Nishida, H. Sasabe, W. Knoll, High Resolution X-Ray Photoelectron Spectroscopy Measurements of Octadecanethiol Self-Assembled Monolayers on Au(111), Langmuir 14 (1998) 2092–2096.
[20] F.P. Cometto, C.A. Calderón, M. Berdakin, P. Paredes Olivera, V.A. Macagno, E.M. Patrito, Electrochemical Detection of the Thermal Stability of n-Alkanethiolate Monolayers on Au(111), Electrochim. Acta 61 (2012) 132–139.
[21] F.P. Cometto, E.M. Patrito, P. Paredes Olivera, G. Zampieri, H. Ascolani, Electrochemical, High-Resolution Photoemission Spectroscopy and vdW-DFT Study of the Thermal Stability of Benzenethiol and Benzeneselenol Monolayers on Au(111), Langmuir 28 (2012) 13624–13635.
[22] N.G. Tognalli, A. Fainstein, C. Vericat, M.E. Vela, R.C. Salvarezza, Exploring Three-Dimensional Nanosystems with Raman Spectroscopy: Methylene Blue Adsorbed on Thiol and Sulfur Monolayers on Gold, J. Phys. Chem. B 110 (2006) 354–360.
[23] E.M. Euti, P. Vélez Romero, O. Linarez Pérez, G. Ruano, E.M. Patrito, G. Zampieri, E.P.M. Leiva, V.A. Macagno, F.P. Cometto, Electrochemical HR-XPS and SERS Study of the Self-Assembly of Biphenyl 4,4′-Dithiol on Au(111) from Solution Phase, Surf. Sci. 630 (2014) 101–108.
[24] J.P. Perdew, K. Burke, M. Ernzerhof, Generalized Gradient Approximation Made Simple, Phys. Rev. Lett. 77 (1996) 3865–3868.
[25] D. Vanderbilt, Soft Self-Consistent Pseudopotentials in a Generalized Eigenvalue Formalism, Phys. Rev. B 41 (1990) 7892–7895.
[26] P. Giannozzi, S. Baroni, N. Bonini, M. Calandra, R. Car, C. Cavazzoni, D. Ceresoli, G.L. Chiarotti, M. Cococcioni, I. Dabo, et al., QUANTUM ESPRESSO: A Modular and Open-Source Software Project for Quantum Simulations of Materials, J. Phys. Condens. Matter 21 (2009) 395502.
[27] H.J. Monkhorst, J.D. Pack, Special Points for Brillouin-Zone Integrations, Phys. Rev. B 13 (1976) 5188–5192.
[28] B.P.U. Graeme Henkelman, A Climbing Image Nudged Elastic Band Method for Finding Saddle Points and Minimum Energy Paths, J. Chem. Phys. 113 (2000) 9901–9904.
[29] S. Plimpton, Fast Parallel Algorithms for Short-Range Molecular Dynamics, J Comput. Phys. 117 (1995) 1–19.
[30] A.C.T. van Duin, S. Dasgupta, F. Lorant, W.A. Goddard, ReaxFF: A Reactive Force Field for Hydrocarbons, J. Phys. Chem. A 105 (2001) 9396–9409.
[31] K. Chenoweth, A.C.T. van Duin, W.A. Goddard, ReaxFF Reactive Force Field for Molecular Dynamics Simulations of Hydrocarbon Oxidation, J. Phys. Chem. A 112 (2008) 1040–1053.
[32] T.T. Järvi, A. Kuronen, M. Hakala, K. Nordlund, A.C.T. van Duin, W.A. Goddard, T. Jacob, Development of a ReaxFF Description for Gold, Eur. Phys. J. B 66 (2008) 75–79.
[33] K. Joshi, A.C.T. van Duin, T. Jacob, Development of a ReaxFF Description of Gold Oxides and Initial Application to Cold Welding of Partially Oxidized Gold Surfaces, J. Mater. Chem. 20 (2010) 10431–10437.
[34] O. Rahaman, A.C.T. van Duin, W.A. Goddard, D.J. Doren, Development of a ReaxFF Reactive Force Field for Glycine and Application to Solvent Effect and Tautomerization, J. Phys. Chem. B 115 (2011) 249–261.
[35] C.-J. Zhong, M.D. Porter, Fine Structure in the Voltammetric Desorption Curves of Alkanethiolate Monolayers Chemisorbed at Gold, J. Electroanal. Chem. 425 (1997) 147–153.
[36] L.-J. Wan, M. Terashima, H. Noda, M. Osawa, Molecular Orientation and Ordered Structure of Benzenethiol Adsorbed on Gold(111), J. Phys. Chem. B 104 (2000) 3563–3569.
[37] F.P. Cometto, V.A. Macagno, P. Paredes-Olivera, E.M. Patrito, H. Ascolani, G. Zampieri, Decomposition of Methylthiolate Monolayers on Au(111) Prepared from Dimethyl Disulfide in Solution Phase, J. Phys. Chem. C 114 (2010) 10183–10194.
[38] M.M. Walczak, D.D. Popenoe, R.S. Deinhammer, B.D. Lamp, C. Chung, M.D. Porter, Reductive Desorption of Alkanethiolate Monolayers at Gold: A Measure of Surface Coverage, Langmuir 7 (1991) 2687–2693.
[39] J. Haddad, H.-G. Steinrück, H. Hlaing, S. Kewalramani, D. Pontoni, H. Reichert, B. M. Murphy, S. Festersen, B. Runge, O.M. Magnussen, et al., Order and Melting in Self-Assembled Alkanol Monolayers on Amorphous SiO_2, J. Phys. Chem. C 119 (2015) 17648–17654.
[40] H. Zhu, A. Dhinojwala, Thermal Behavior of Long-Chain Alcohols on Sapphire Substrate, Langmuir 31 (2015) 6306–6313.
[41] X. Xiao, B. Wang, C. Zhang, Z. Yang, M.M.T. Loy, Thermal Annealing Effect of Alkanethiol Monolayers on Au(111) in Air, Surf. Sci. 472 (2001) 41–50.
[42] S.W. Joo, S.W. Han, K. Kim, Adsorption of 1,4-Benzenedithiol on Gold and Silver Surfaces: Surface-Enhanced Raman Scattering Study, J. Colloid Interface Sci. 240 (2001) 391–399.
[43] H.S. Kato, J. Noh, M. Hara, M. Kawai, An HREELS Study of Alkanethiol Self-Assembled Monolayers on Au(111), J. Phys. Chem. B 106 (2002) 9655–9658.
[44] A. Kudelski, Characterization of Thiolate-Based Mono- and Bilayers by Vibrational Spectroscopy: A Review, Vib. Spectrosc. 39 (2005) 200–213.
[45] P.E. Laibinis, G.M. Whitesides, D.L. Allara, Y.T. Tao, A.N. Parikh, R.G. Nuzzo, Comparison of the Structures and Wetting Properties of Self-Assembled Monolayers of N-Alkanethiols on the Coinage Metal Surfaces Copper, Silver, and Gold, J. Am. Chem. Soc. 113 (1991) 7152–7167.
[46] W. Fabianowski, L.C. Coyle, B.A. Weber, R.D. Granata, D.G. Castner, A. Sadownik, S.L. Regen, Spontaneous Assembly of Phosphatidylcholine Monolayers via Chemisorption onto Gold, Langmuir 5 (1989) 35–41.
[47] J.F. Moulder, W.F. Stickle, P.E. Sobol, K.D. Bomben, Handbook of X-Ray Photoelectron Spectroscopy, Physical Electronics, Eden Prairie, MN, 1995.
[48] J.A. Rodriguez, J. Dvorak, T. Jirsak, G. Liu, J. Hrbek, Y. Aray, C. González, Coverage Effects and the Nature of the Metal-Sulfur Bond in S/Au(111): High-Resolution Photoemission and Density-Functional Studies, J. Am. Chem. Soc. 125 (2003) 276–285.
[49] R. Yamada, H. Wano, K. Uosaki, Effect of Temperature on Structure of the Self-Assembled Monolayer of Decanethiol on Au(111) Surface, Langmuir 16 (2000) 5523–5525.

[50] R. Yamada, H. Sakai, K. Uosaki, Solvent Effect on the Structure of the Self-Assembled Monolayer of Alkanethiol, Chem. Lett. 28 (1999) 667–668.
[51] M.S. Al-Abdul-Wahid, C.-H. Yu, I. Batruch, F. Evanics, R. Pomès, R.S.A. Prosser, Combined NMR and Molecular Dynamics Study of the Transmembrane Solubility and Diffusion Rate Profile of Dioxygen in Lipid Bilayers, Biochemistry (Mosc.) 45 (2006) 10719–10728.
[52] M.S. Al-Abdul-Wahid, F. Evanics, R.S. Prosser, Dioxygen Transmembrane Distributions and Partitioning Thermodynamics in Lipid Bilayers and Micelles, Biochemistry (Mosc.) 50 (2011) 3975–3983.
[53] H.H. Schobert, The Chemistry of Hydrocarbon Fuels, Butterworth-Heinemann, 2013.
[54] F.A. Soria, P. Paredes-Olivera, E.M. Patrito, Chemical Stability toward O_2 and H_2O of Si(111) Grafted with CH_3 $CH_2CH_2CH_3$, $CHCHCH_3$, and $CCCH_3$, J. Phys. Chem. C 119 (2015) 284–295.
[55] F.P. Cometto, P. Paredes-Olivera, V.A. Macagno, E.M. Patrito, Density Functional Theory Study of the Adsorption of Alkanethiols on Cu(111) Ag(111), and Au (111) in the Low and High Coverage Regimes, J. Phys. Chem. B 109 (2005) 21737–21748.
[56] B.N. Jariwala, C.V. Ciobanu, S. Agarwal, Initial Oxidation Stages of Hydrogen- and Styrene-Terminated Si(100) Surfaces: A Molecular Dynamics Study, Surf. Sci. 605 (2011) L61–L66.